3 April 2025

ISCI 1A24

Devil Facial Tumour Disease Treatment with Vincristine:

Investigating Semi-Resistance in Transmissible Cancers through Cell Mechanics

Group 13

Sulagna Nandi, Nam Nguyen, Sara Osman, Ann Phillip, Keira Sponagle

Abstract

Devil Facial Tumour Disease (DFTD) is a highly transmissible cancer observed in *Sarcophilus harrisii*, the Tasmanian devil, and is responsible for severe population declines in its native land of Tasmania, Australia. Originating from Schwann cells, DFTD causes tumour growth on the neck and facial regions of Tasmanian devils. The disease is fatal, leading to death through metastasis, infection of open wounds, or anorexia. The first phase of this study examined the efficacy of chemotherapeutic drugs in treating DFTD, focusing on vincristine. Two linear regression models were employed to analyze tumour growth with and without drug administration. The regression-based study discovered a correlation between the presence of chemotherapeutic drugs and tumour cell growth: the presence of the drug was observed to prevent excessive tumour cell division, while its absence suggested unregulated tumour growth. These conclusions were drawn based on the regression lines of both models. The model representing initial and final cell counts of vincristine-treated tumours had a positive slope, but the R^2 value of 0.980 indicated a strong predictability of the final cell count with respect to the initial. Conversely, the final DFTD cell count in untreated tumours was unpredictable, with little to no correlation to the initial cell count and an R^2 value of 0.006. This regression analysis concluded that while vincristine regulated tumour cell proliferation, it did not induce cell death, suggesting semi-resistance. Based on this semi-resistance, the proposed study investigates the biophysical mechanisms within DFTD cells. Specifically, it aims to explore how vincristine affects cytoskeletal integrity as a potential source of this resistance. Using principles of biophysics, cell stiffness will be examined to determine whether there is a correlation between chemotherapeutic stress and the DFTD cells' ability to maintain cytoskeletal structural integrity. Additionally, the processes involved in potential cytoskeletal restructuring will be further analyzed by measuring choline metabolism, an indicator of cytoskeletal repair. By integrating biophysical and

biochemical analyses, this study aims to uncover the mechanisms underlying vincristine's limited effectiveness against DFTD. Understanding how DFTD cells maintain cytoskeletal integrity under chemotherapeutic stress could provide critical insights into overcoming drug resistance. These findings may contribute not only to improving treatment strategies for DFTD but also to a broader understanding of cancer cell mechanics, potentially informing therapies for other cancers with similar resistance mechanisms.

General Introduction and Background

The Tasmanian devil (*Sarcophilus harrisii*) is the largest extant marsupial carnivore, native to the island of Tasmania in Australia.[1] This species has suffered severe population declines of up to 80% due to the emergence of DFTD, a unique and highly transmissible cancer of Schwann cell origin. Schwann cells, a type of glial cell found in the peripheral nervous system, are responsible for producing myelin, which insulates axons and allows for the quick transmission of electrical impulses in neurons.[2] DFTD is identified both morphologically and by the expression of periaxin, a myelin-associated protein.[3]

Since its first documentation in 1997, DFTD has spread through fighting behaviour like biting, as well as feeding.[4] Due to the nature of these interactions, DFTD spread is heightened during mating season. Notably, gender does not influence susceptibility; however, older devils are more at risk, likely due to increased exposure during mating and competition.[4]

DFTD is a neoplastic condition, meaning it results from abnormal and excessive growth of tissue.[4] DFTD is characterized by the growth of undifferentiated soft tissue tumors that typically originate in the facial and neck regions.[5] These tumors have high rates of metastasis (65%) and frequently spread to regional lymph nodes and visceral organs.[4] Despite the presence of a layer of tissue around the tumour called the

pseudocapsule, the tumour progresses quickly, pushing on surrounding tissue. The disease ultimately leads to death within six months of symptom onset due to starvation, metastatic complications or other factors.[5] In 2008, the Tasmanian devil was officially classified as an endangered species due to the devastating impact of DFTD.[1] Given the urgency of DFTD's impact on Tasmanian devil populations, researchers have explored various treatment strategies, including the use of chemotherapeutic agents.

In recent literature, no definitive treatment for DFTD has been established. Chemotherapeutic trials in 2015, testing vincristine, doxorubicin, and carboplatin, found no significant difference in survival time between treated and untreated devils.[6] In contrast, endeavours into immunization strategies have shown promise.[7] Small-scale trials on captive devils demonstrated immune-mediated tumour regression, and larger trials found that 95% of immunized devils developed an anti-DFTD antibody response. Despite progress in immunotherapy, understanding of DFTD remains incomplete, particularly regarding the mechanical properties of tumour cells. Across cancer research, biochemical signalling in aggressive tumours is well-studied, but the mechanical signals – forces exerted by and on tumour cells – are less understood.[8] Recent studies have begun exploring mechanotransduction, the process by which mechanical forces influence gene expression and cytoskeletal integrity. Cytoskeletal analysis of cells undergoing chemotherapeutic treatments has been done on solid tumors, including human breast cancer and orthotopic fibrosarcoma in mouse models, revealing that nanomechanical data can be used to understand cancer progression and the impact of chemotherapeutic treatment.[9] Given that previous chemotherapy trials for DFTD showed no significant improvement in survival, understanding how vincristine affects the mechanical properties of DFTD cells may provide insight into why conventional chemotherapy has been

ineffective. By bridging the gap between biochemical and mechanical perspectives in cancer research, our study offers a novel approach to evaluating DFTD treatment.

The goal of the computational study was to investigate the efficacy of chemotherapeutic agents commonly used to treat cancer on DFTD. The second part of our study builds off of this analysis, investigating why the chosen chemotherapeutic agent, vincristine, fails to work against DFTD, with hopes of opening avenues to effective treatments that bypass the barriers found. The proposed study poses this question from a biophysical perspective in order to investigate cell mechanics involved in DFTD, an area not well-researched currently. This study investigates cellular structure, as vincristine's mechanism of action targets microtubules, which play a crucial role in maintaining cell shape, intracellular transport, and mitotic division. This perspective and the chosen methods will answer how vincristine treatment affects cytoskeletal integrity and what restructuring we are able to detect by tracking choline metabolism.

Vincristine Background

Vincristine (Figure 1) is a vinca alkaloid that disrupts microtubules and induces apoptosis in rapidly dividing cells.[10] Its mechanism of action is stopping the cell cycle by acting on microtubule dynamics in the mitosis phase of cell division and proliferation, causing cell cycle arrest in metaphase. The binding site for vincristine is located at the beta-subunit on the boundary between the two tubulin heterodimers that make up microtubules. By binding to both heterodimers, vincristine splits the microtubule fibres. As the fibres rejoin in irregular order, often attached through vincristine, they fail to properly function in mitotic spindle formation. This disruption prevents chromatid separation, leading to cell cycle arrest, as well as an altered cytoskeleton.[11] In most cases, this alteration is in the form of cytoskeletal weakening, impairing cellular integrity and function.

Cell cycle arrest will lead to apoptosis via the p53 pathway. The p53 tumor suppressor pathway is activated by mitotic arrest when DNA damage and spindle assembly defects are detected.[12] Pro-apoptotic genes like BAX and PUMA are initiated, culminating in programmed cell death. Additionally, vincristine-induced microtubule destabilization can compromise mitochondrial integrity, causing cytochrome c release in the cytosol.[13] This activates caspase-9, which in turn triggers a cascade of effector caspases that drive apoptosis.

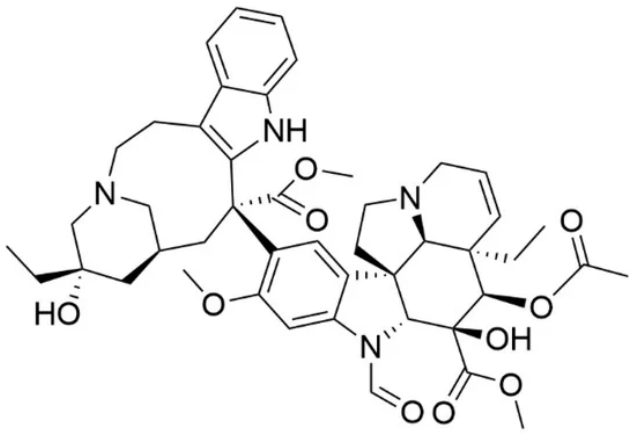

Figure 1: Vincristine's chemical structure.[10]

As this drug inhibits tubulin from forming functional microtubules in rapidly dividing cells, it is best classified as a microtubule inhibitor.[14] Using traditional receptor-based classification, vincristine's mode of action would therefore be as an exogenous functional antagonist.

Vincristine is not lipid soluble, and so cannot pass through the phospholipid membrane.[15] It is large and positively charged, and can reach intracellular structures – the microtubules – through active transport, with the help of liposomes. In therapeutics, vincristine is often delivered using liposomal formation encapsulations to prevent degradation, improve stability, and increase its accumulation in tumor tissues.

Vincristine's chemical structure (Figure 1) plays a key role in its mechanism, mode, and method of action. As a bisindole alkaloid, its two fused indole rings facilitate hydrophobic interactions with beta-tubulin, stabilizing its binding at the tubulin interface and preventing proper microtubule polymerization.[16,17] Indole-based tubulin inhibitors have hydrogen bonding interactions between their methoxy and hydroxyl groups and amino acids in tubulin, allowing for vincristine's high-affinity bonding.[17] The protonation of one of the two tertiary nitrogens in vincristine affects its solubility and transport,[18] corresponding to its method of action.

Vincristine has shown limited success in previous studies on DFTD, with evidence indicating poor efficacy in reducing tumors.[6,19] However, the underlying mechanisms behind this inefficacy are still unknown. Given vincristine's established role in treating cancers of other systems, it is critical to investigate whether its failure in DFTD is due to inherent resistance mechanisms, differences in cytoskeletal organization, or alternative pathways that allow the cell to remain viable. This study investigates cytoskeletal integrity in a way that could inform novel therapeutic strategies by offering insight into why conventional chemotherapies have been ineffective, guiding future treatment approaches.

Motivations and Study Approach

Emerging infectious diseases in wildlife are widely acknowledged as a significant global conservation threat.[20] However, the impact of DFTD on the Tasmanian devil population is particularly severe, leading to drastic population declines and threatening the species with potential extinction.[21] The disease spreads through direct contact, exploiting the devils' social behaviors, and its near 100% mortality rate raises urgent concerns for conservation efforts.

There are two distinct forms of DFTD identified as DFT1 and DFT2.[22] DFT1 and DFT2 are genetically different and originated independently, so though they are both transmissible cancers affecting Tasmanian devils, they are separate diseases. DFT1, first identified in 1996, is the dominant form and is believed to have arisen from a female devil. DFT2, discovered in 2014, is genetically distinct and likely originated from a male devil. The occurrence of two distinct cancer forms with similar pathological mechanisms in Tasmanian devils underscores their susceptibility to this type of disease due to their mating behaviours and lack of an immune response.

In Tasmania, DFT1 was first detected on the North-East coast and spread southwest across the majority of the state, though the spread exhibits dispersal limitation due to physical environmental barriers (Figure 2).[23] Geographical barriers like mountains and rivers briefly impeded the spread, making the northwest and southwest of Tasmania the only places believed to be currently free of DFT1. DFT2 was first detected in the southeast of Tasmania, in the D'Entrecasteaux Peninsula region, and remains localized there as the area is surrounded by mountain ranges and sea. Since our study focuses on the spread and effects of DFT1 specifically, Figure 2 will model its geographic spread through the island and the severity of the spread. If no action is taken regarding the spread of the disease, DFTD is predicted to affect the entire island and cause the extinction of the species.[21]

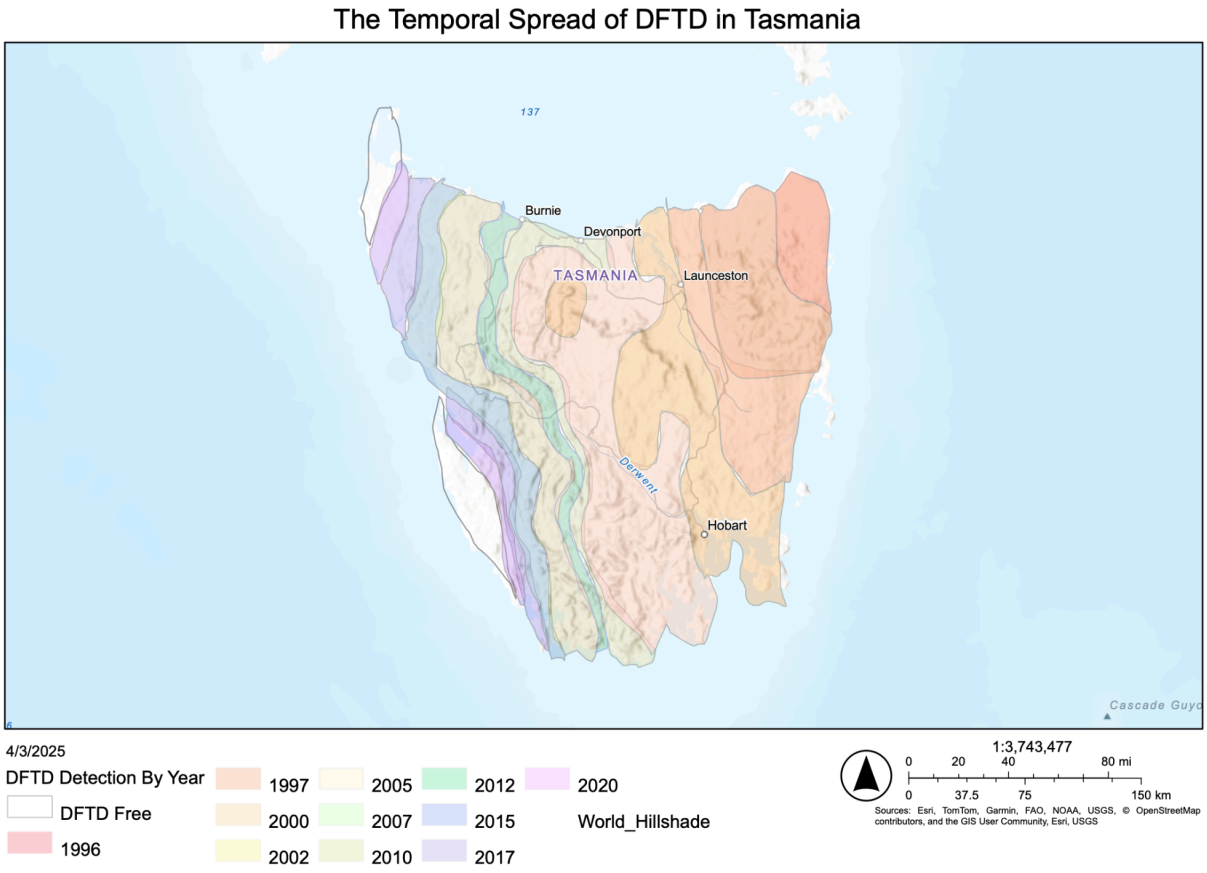

Figure 2: Geographical distribution and temporal spread of DFTD across Tasmania. The map shows the westward movement of DFTD from its initial detection in North-East Tasmania in 1996. Areas are colour coded by year of first detection, indicating the expansion of the disease over time. The map was created using quantitative and geographic data from Patchett at al. 2020 and Cunningham et al. 2021.[7,11]

The extinction of the Tasmanian devil would have cascading ecological consequences, disrupting predator-prey dynamics and altering community structure. As apex scavengers and mesopredators, Tasmanian devils exert top-down control on populations of smaller carnivores, such as feral cats and invasive red foxes, which prey on smaller marsupials.[24] The loss of Tasmanian devils threatens predator-mediated competition, shifting community dynamics. As Tasmanian devil populations decline,

these mesopredators can increase in density, intensifying interspecific competition and amplifying predation pressure on vulnerable species. This may result in further local population declines and potential extinctions. Additionally, DFTD itself represents an ecological disturbance, reshaping species interactions and triggering shifts in community composition. These broader ecological effects underscore the urgency of conservation efforts, as the loss of the Tasmanian devil would destabilize Tasmania's ecosystem.

Devil Facial Tumour Disease (DFTD) poses a critical threat to Tasmanian devil populations, with its rapid transmission and high mortality rate leading to severe population declines.[1] Despite extensive research into DFTD's pathology, effective treatment options remain limited. Understanding how this transmissible cancer responds to chemotherapy is essential for assessing its potential as a viable treatment strategy. However, prior studies have suggested that some chemotherapeutic agents, including vincristine, show limited or no efficacy against DFTD.[19] This raises important questions about the tumour's unique cellular properties and its resistance to certain drugs.

Our grant proposal will include two studies. The first study evaluates whether widely used chemotherapeutic agents, specifically vincristine, are effective in treatment of DFTD via a computational analysis. By assessing tumour response to these drugs, we can determine if conventional chemotherapeutic agents offer a feasible solution to DFTD. This study is crucial for identifying potential treatments and understanding the general susceptibility of DFTD cells to chemotherapeutic agents.

The proposed study uses these findings to inform its objectives. The goal of this second study is to investigate why vincristine, a widely used chemotherapeutic drug, fails to work against DFTD. Given that vincristine disrupts microtubule polymerization, we hypothesize that DFTD cells may exhibit unique

cellular properties that influence drug resistance.[14] By analyzing cell stiffness and structural integrity in response to vincristine treatment, this study aims to determine whether altered dynamics in cellular structure contribute to treatment failure. Understanding these cellular properties is critical, as it may reveal broader mechanisms of resistance and inform future drug development tailored to DFTD.

Computational Analysis: Methods

This study applied linear regression modelling to examine the impact of a chemotherapeutic agent on tumour cell counts. Linear regression is a statistical method used to describe the relationship between two variables by fitting a line that best represents the data. The objective is to minimize the difference between the actual data points and the predicted values on the line. This is achieved by reducing the mean squared error (MSE), which gives the mean squared distance between the observed and predicted values. Through the use of multivariable calculus, the slope and y-intercept of the line were determined by calculating the partial derivatives of the MSE function with respect to these parameters and equating them to zero, observed in Equations 1 to 3. This process identifies the line that produces the smallest overall error.

$$MSE(m, b) = \frac{1}{n}\sum_{i=1}^{n} (y_i - (mx_i + b))^2 \quad (1)$$

$$\frac{\partial MSE}{\partial m} = 0 \quad (2)$$

$$\frac{\partial MSE}{\partial b} = 0 \quad (3)$$

The relationship between the final cell count and the number of DFTD cells (Devil Facial tumour Disease cells) was modelled using simple linear regression. The model follows Equation 4:

$$y = mx + b \quad (4)$$

In Equation 4, y represents the final cell count, x denotes the number of DFTD cells, m is the slope (indicating how much the final cell count changes for each additional DFTD cell), and b is the y-intercept (the predicted final cell count when no DFTD cells are present). The R-squared (R^2) value was used to evaluate the model's accuracy. This metric indicates how much of the variation in the final cell count can be explained by the number of DFTD cells. An R^2 value close to 1 indicates a strong fit, whereas a value near zero suggests little to no relationship.

Two models were generated: one for the condition where vincristine was administered and another for the condition where it was not. For both cases, the line of best fit, along with the slope, y-intercept, and R^2 value, was calculated to assess the effectiveness of the drug in influencing tumour cell proliferation.

Computational Analysis: Results

The results indicate a distinct difference in tumour cell behaviour based on the presence or absence of vincristine. In the condition where vincristine was administered, a strong and consistent linear relationship was observed between the number of DFTD cells and the final cell count. The line of best fit for this scenario is represented by Equation 5, while the data is plotted in Figure 3.

$$y = 0.9638x + 261.39 \quad (5)$$

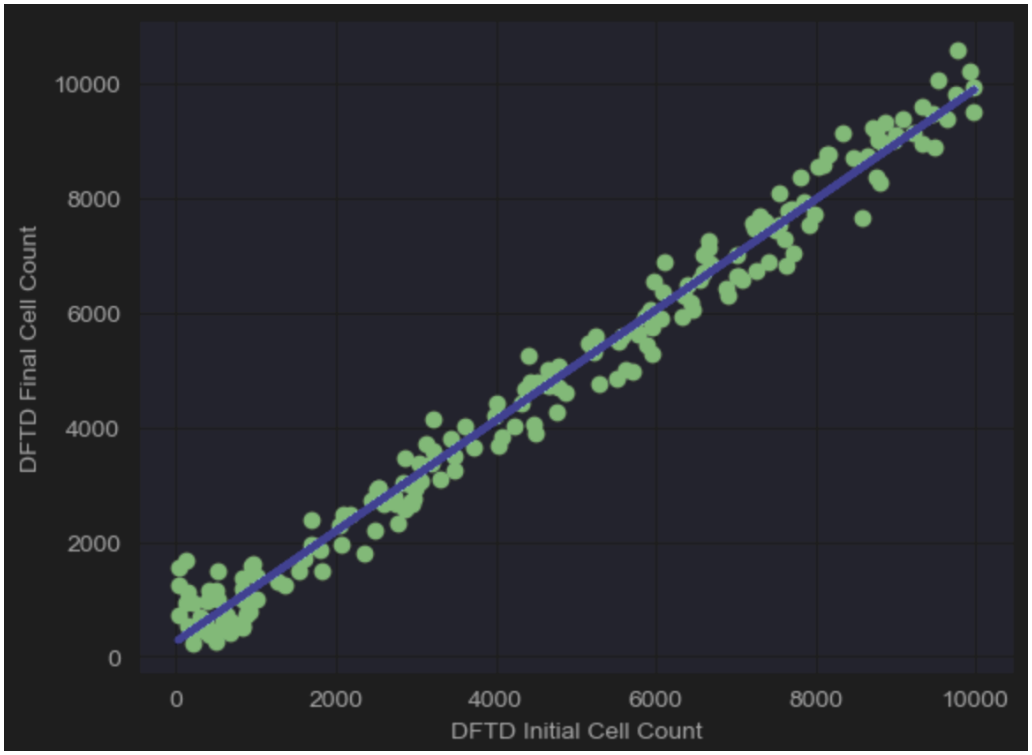

Figure 3: Initial and final DFTD tumour cell count in 192 Tasmanian devils with Vincristine treatment. There is a clear trend showing that Vincristine use is correlated with tumours remaining the same size rather than going through uncontrolled growth.

The slope of approximately 0.96 indicates that for each additional DFTD cell, the final cell count increases by nearly one cell. This close-to-one relationship suggests that the chemotherapeutic agent effectively prevents excessive tumour cell division, keeping the final cell count proportional to the number of DFTD cells.

The y-intercept of approximately 261.39 does not represent the final cell count when there are no DFTD cells, as this would be biologically implausible. Instead, it reflects the average deviation from the perfectly linear relationship due to biological variability and noise in the data. This means that, given an initial DFTD cell count, the final count increases by approximately 261 cells on average, but not always

precisely by this amount. This statistical offset accounts for factors such as baseline noise, variations in cell behaviour, or slight inconsistencies in the measurement process.

The R^2 value of approximately 0.980 indicates an exceptionally strong fit, with 98 percent of the variation in the final cell count explained by the number of DFTD cells. This strong correlation suggests that the chemotherapeutic agent inhibits mitotic activity, preventing the tumour cells from undergoing uncontrolled division. The near-perfect linear relationship indicates that the drug enforces a predictable and limited tumour cell count, preventing unchecked proliferation.

The drug's effectiveness is likely due to its antimitotic properties. Antimitotic drugs target the mitotic spindle apparatus, which is essential for cell division. By disrupting microtubule dynamics or interfering with spindle assembly, these agents halt mitosis, leading to cell cycle arrest and, eventually, cell death. According to some studies, antimitotic drugs are widely used in cancer treatment due to their ability to selectively target rapidly dividing cells, thereby limiting tumour growth.[25]

In contrast, the condition without vincristine treatment exhibited high variability and an absence of a clear linear trend. Equation 6 displays the line of best fit for this scenario and Figure 4 shows the plot.

The slope of approximately -8.1 indicates a slight negative relationship; however, this value lacks biological significance due to the extreme scatter in the data. The R^2 value of approximately 0.006 indicates an almost nonexistent correlation, meaning that the number of DFTD cells offers no predictive value for the final cell count. The high variability and weak relationship suggest that, in the absence of vincristine, the final cell count is essentially unpredictable. This result is indicative of unregulated tumour

growth, where the final cell count is influenced by random factors rather than a consistent relationship with the initial DFTD cell count.

$$y = -8.1052x + 569453.25 \quad (6)$$

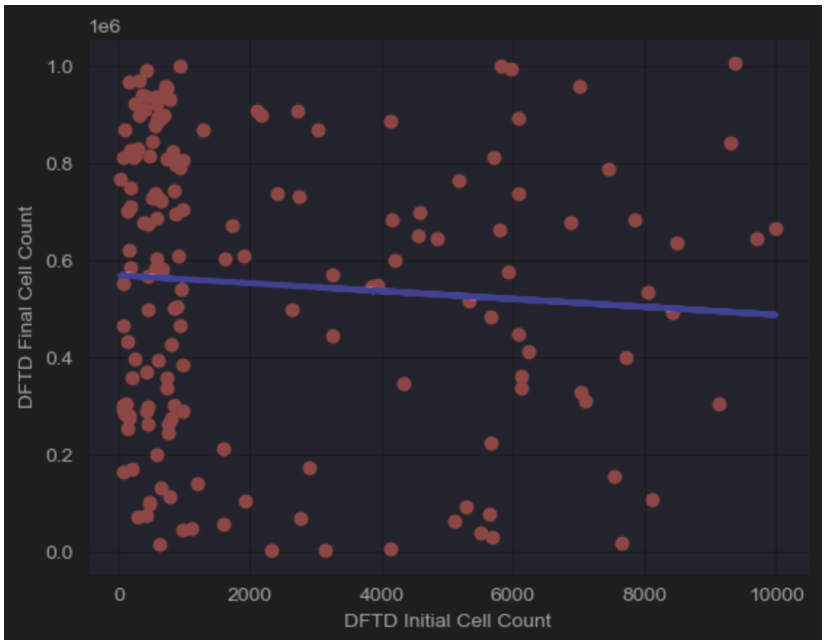

Figure 4: Initial and final DFTD tumour cell count in 168 Tasmanian devils without any treatment. There is no clear relationship between initial DFTD cell count and final DFTD cell count and there is uncontrolled growth in many cases.

Overall, the results demonstrate that vincristine does not reduce the cell count, but it still exerts a strong antimitotic effect, maintaining a stable and predictable final cell count. Without the drug, tumour growth appears chaotic and highly variable, with no discernible pattern.

Proposed Cytoskeletal Analysis Study: Motivations

The computational analysis performed determined that DFTD cells are partially resistant to vincristine treatment; treated cells will continue to proliferate, but in a controlled and predictable manner proportional to their initial cell count. Conversely, untreated tumours have marked increases in cell counts that are unpredictable. Thus, DFTD cells exhibit ‘semi-resistance’ to vincristine: while the drug does not induce cell death, it regulates proliferation, leading to a more stable cancer state. Though relevant to DFTD in general, this study will focus solely on DFT1 cells. We cannot group together findings between DFT1 and DFT2 due to the differences in their gross morphology that could create a discrepancy in baseline values.[26] Instead, focusing on DFT1 is sensible as it is more prevalent, both in numbers and in geographic distribution. Eliminating this confounding variable allows for more accurate findings. With this knowledge and the findings of the regression analysis, our proposed study focuses on investigating the semi-resistance of DFT1 cells to vincristine from a biophysical perspective in order to further our exploration of chemotherapeutic agents and DFTD.

Specifically, we ask: How does vincristine alter cell stiffness in DFT1 cells and what changes in choline metabolism contribute to the cell’s response to vincristine treatment? This question is multifaceted and allows an exploration into the cells’ biomechanical properties and their ability to recover from external stresses. We will investigate whether the DFT1 cells’ evasion of apoptosis lies in their biomechanical response and what metabolic and mechanical indicators can explain vincristine’s apparent ability to tame DFTD cell proliferation. By examining both cell stiffness and metabolic adaptations, we aim to determine whether DFT1 cells’ resistance to vincristine-induced apoptosis is linked to their ability to maintain or restore cytoskeletal integrity under chemotherapeutic stress.

In order to determine the relevance of cytoskeletal integrity in DFT1 cells' semi-resistance to vincristine, we will focus on vincristine's mechanism of action. As discussed in the Vincristine Background, vincristine disrupts the microtubules in the cytoskeleton, leading to cell cycle arrest.[14] Prolonged mitotic arrest in some cells triggers mitotic catastrophe, leading to apoptosis, however, semi-resistant cells like DFTD are able to escape apoptosis.[27] A hypothesized route for this evasion is through activating repair mechanisms to maintain cytoskeletal integrity.[11] Vincristine treatment has been shown to decrease cell stiffness through its disruption of microtubules in other cancers, and it is hypothesized that the cytoskeletal repair mechanism counters that.[28] As the cytoskeleton repairs itself during and after therapeutic administration, choline is metabolized in the cell.[29,30] Therefore, the measurable changes that indicate an initially successful treatment and the cells' attempt to defend themselves against this treatment are a weakened cytoskeleton and the production of choline metabolites, respectively.

Proposed Cytoskeletal Analysis Study: Methods

Overview, Importance, and Novelty

Atomic Force Microscopy (AFM) will be used to assess the mechanical properties of DFT1 cells undergoing vincristine treatment to explore its efficacy. Nanoindentation, a subset of AFM, uses a small probe to measure the displacement made from a given force (Figure 5), generating comparative stiffness values.[31] The treatment's efficacy will be based on the observed cytoskeletal weakening after administration.[11] While AFM has been used to understand the cell mechanics during and after chemotherapy in other cancers,[32–34] this technique has not yet been applied to DFTD and vincristine. Importantly, this study will focus on uncharted areas in cancer science and investigate the cytoskeleton's role in semi-resistant cell types. The measurements collected from nanoindentation will focus on changes

in cell stiffness, exploring the effects of vincristine treatment on cytoskeletal integrity in successful and unsuccessful cases.[31]

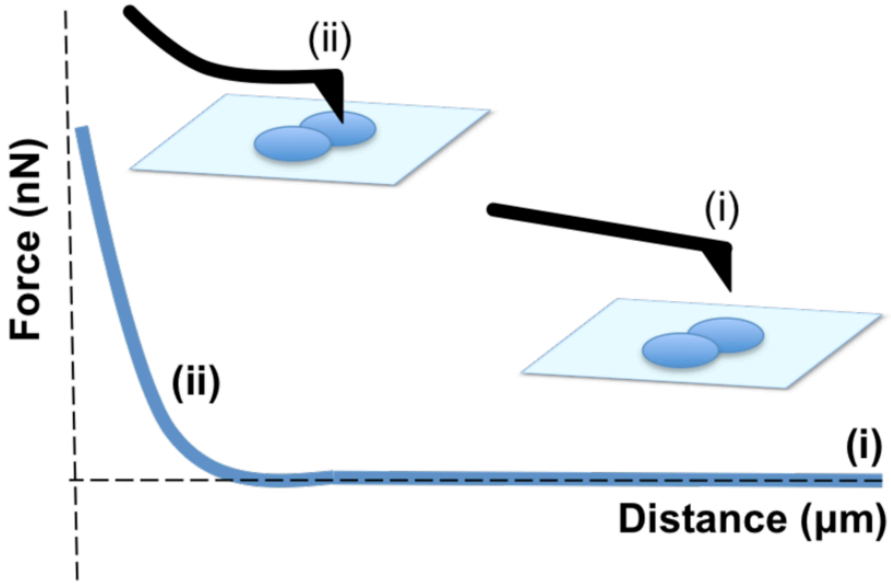

Figure 5: Nanoindentation process, shown above the axes, on individual cells. A force-distance graph is shown below, where (i) corresponds to the non-contact phase (approach or removal) and (ii) represents when the probe is in contact with the cell. Our study will generate 3 force-distance curves per cell, measuring 30 cells per experimental group. Each force-distance curve produces a Young's modulus, which will be simplified into a single modulus per cell, giving 30 Young's moduli per experimental group.

Magnetic Resonance Spectroscopy (MRS) will be used to further the experimental outcomes of this study by providing context to the AFM findings. By exploring metabolic shifts associated with vincristine treatment in susceptible and semi-resistant cells, the underlying cellular mechanisms behind resistance can be investigated. Choline metabolism increases when the cytoskeleton is being remodelled, and MRS offers a way to track the resulting metabolites.[35] The application of MRS in this study will focus on analyzing total choline (tCho) magnetic resonance spectral peaks and observing how they change over time following the administration of vincristine. Integrating the area under each peak can give us an

approximation of how much tCho is present. The exact values are not important as we are interested in the relativistic changes in tCho. Combining this data with AFM observations ensures a more complete understanding of results, enabling more reliable interpretations. Stiffened DFT1 cells (measured using AFM) accompanied by increased choline metabolism would indicate that the actin cortex is reinforcing, repairing the cytoskeleton, and likely playing a part in DFTD's partial resistance to vincristine.[36] MRS has been used extensively to monitor membrane metabolism during treatment, providing insight to cellular response to chemotherapy. While previous studies have linked choline metabolites to membrane integrity throughout treatment,[37–39] their role in cytoskeletal repair remains less explored. This study will leverage MRS to investigate the metabolic adaptations of vincristine-treated cells, offering a novel perspective on how DFTD cells maintain cytoskeletal integrity under chemotherapy-induced stress.

Neuroblastoma cells will be used as a comparative model in order to determine the effects of vincristine treatment on DFT1 cells. Vincristine treatment successfully induces apoptosis in human neuroblastoma cells[13] and so the effects of vincristine on susceptible cells can be compared to its effects on DFT1 cells. As well, neuroblastoma and DFTD cells have similarities as they are both aggressively metastasizing Schwann cells of neural crest origin.[34] Furthermore, neuroblastoma cells are easily accessible, making them a practical choice for this study. Tu et al. observed neuroblastoma cells treated with vincristine, which were found to undergo apoptosis in the first 24 hours of treatment, with measurements taken every 6 hours.[13] However, it is important to note that second waves of apoptosis (caspase-independent cell death) have also been shown to occur within 48 hours.[40] We will model our study based on these findings, collecting data before vincristine treatment, and then after 6, 12, 18, 24, and 48 hours of continuous

vincristine administration for both the DFT1 and neuroblastoma cells. This gives data across six different time marks and ensures the completeness of our data set.

The vincristine used will be in the range of 10 to 20 nM, as substantiated by the protocol of Tu et al.[13] This concentration allows for observable cytoskeletal changes, while still maintaining some viable cells for metabolic studies. To account for the difference between neuroblastoma cells and DFT1 cells, a preliminary dose-response assessment will occur using AFM and MRS to ensure the cell viability at multiple time points for a given concentration. The 10 to 20 nM range provided by Tu et al. provides an educated starting point for this assessment.

The vincristine will remain in the culture medium throughout the entire treatment period (6, 12, 18, 24, or 48 hours). No washout or removal of vincristine will occur between time points, ensuring sustained drug exposure. This method mirrors the process of Tu et al., as well as the continuous chemotherapy regimen commonly used in clinical settings.[13] By employing continuous vincristine exposure in this study, we can observe the persistent cellular responses to vincristine over time.

This study will use control groups of both DFT1 and neuroblastoma cells to verify that any observations in cell stiffness and tCho change can be accurately attributed to the treatment. Observations of untreated DFT1 cells and untreated neuroblastoma cells will take place after 6, 12, 18, 24, and 48 hours post cell preparation. If variations in cell stiffness and tCho levels in these groups are similar to those observed in their respective experimental groups, we will have to reconsider the significance of the results found.

Cell Line Sourcing and Preparation

In order to perform the study, DFT1 cells will be sourced from the University of Tasmania Central Animal House, which we will be working in partnership with, and human neuroblastoma cells will be sourced from the American Type Culture Collection. In accordance with the preparation methods established by Pinfold et al.,[41] DFTD cell line C5065 will be placed in the RPMI-10FCS medium: RPMI-1640 medium supplemented with 10% fetal calf serum, 5 mM 1-glutamine, and 40 mg/mL of gentamicin. The culture will be kept in a 5% CO_2 incubator at 35°C and full humidity until 90% confluence is reached. The neuroblastoma cells will be prepped in accordance with the methods of Kaya et al. and adapted for MRS analysis according to the Peet et al. protocol.[42,43] SH-SY5Y, the neuroblastoma cell line used by Tu et al.,[13] will be placed in a medium of DMEM F12 (sourced from ThermoFisher) and 10% Nu-serum. The culture will be kept in a 5% CO_2 incubator at 35°C and full humidity until 90% confluence is reached.

The DFT1 and neuroblastoma cells will be continuously exposed to vincristine and measured after 6, 12, 18, 24, and 48 hours. The control DFT1 and neuroblastoma cell groups will not undergo vincristine treatment, but will be prepared with the same methods as the treated groups, in order to evaluate the significance of any observations. Once cultured, cells measured by AFM will be seeded on glass coverslips and immediately placed in a vincristine-containing medium, where they will be incubated continuously for 6, 12, 18, 24, or 48 hours before measurement.[44] These coverslips will then be analyzed directly. Cells to be analyzed using MRS will remain in the vincristine-containing medium for the entire exposure period (6, 12, 18, 24, or 48 hours) before being harvested.

AFM and MRS Methods

The cell stiffness measurements will be taken using an Asylum MFP3D-Bio AFM.[49] A soft cantilever probe (0.006 N/m) with a spherical tip (10 micrometre diameter) will be used to minimize cell damage while still generating detectable deflection. The probe will move at a speed of 5 micrometres/second so that the contribution of hydrodynamic effects can be minimized. The force spectroscopy mode on the AFM will be used to generate force-distance curves at three locations around the cell in order to collect reliable and complete data. For each cell type at each time increment, 30 cells will be measured. The force-distance curves are then analyzed to derive Young's modulus – a metric used to compare stiffness values based on nanoindentation findings – of each.[50] In order to determine the Young's moduli, Hertz's contact model (Equation 7) is used, where F is the indentation force, E is the Young's modulus, v is the Poisson's ratio, R is the radius of the spherical probe tip, and delta (δ) is the distance (indentation depth).[50] The Poisson ratio used in this study is 0.5, which is used for most cancer cells as they are assumed to be nearly incompressible due to high water content.[51] One Young's moduli will be generated per cell from the three force-distance curves. Young's moduli of cells in each condition (time and cell type) will then be compared to their baseline values and then to one another, investigating how vincristine treatment affects cytoskeletal integrity in DFT1 and neuroblastoma cells.

$$F = \frac{4}{3}\frac{E}{(1-\nu^2)}\sqrt{R\delta^3} \tag{7}$$

MRS will be used to investigate choline metabolism in DFT1 and neuroblastoma cells during vincristine treatment. In each condition, 12 samples will be analyzed in order to minimize variability. Once the cells have been prepared appropriately, a high resolution proton MRS will be conducted using a 600 MHz NMR spectrometer.[52] Spectra will be acquired at a controlled temperature of 25°C to maintain consistency

across samples. The spectral region of interest will focus on the choline peak at 3.2 ppm, corresponding to choline-containing compounds involved in phospholipid metabolism.[53] Quantitative analysis will involve integrating the area under the choline peak to determine tCho levels. Comparative analysis of tCho levels over the treatment time course will reveal metabolic alterations associated with vincristine exposure. Elevated tCho levels have been linked to increased membrane turnover and cellular proliferation, while changes in choline metabolism have been associated with tumor progression and treatment resistance. Further discussion and justification of the MRS techniques used in this study can be found in the Imaging and Spectroscopy section of the proposal.

Collected Data

In all, this study will collect comparative stiffness values (Young's moduli) derived from force-distance curves from the AFM measurement, and tCho levels from the MRS measurement. Between the two control groups and two experimental groups measured at six time marks, this study will encompass 24 conditions. For AFM measurements, 720 cells will be analyzed, measuring in triplicate to give 2 160 force-distance curves. These curves will be combined to give 720 Young's moduli, which can then be compared directly. In the MRS data collection, 12 subjects will be analyzed per experimental group, giving 288 comparative tCho values.[54] The layered study approach and robust data set allows for valuable insight into cell mechanics and metabolism.

Conclusions from this Study

This study aims to investigate the role of cytoskeletal adaptation in DFTD's partial resistance by integrating AFM and MRS technologies. By analyzing changes in cell stiffness (Young's modulus) and

choline metabolism (tCho levels), we will assess whether vincristine-treated DFT1 cells reinforce their cytoskeleton to counteract treatment or if the drug successfully induces cytoskeletal destabilization as it avoids apoptosis. As shown in Table 1, this study will allow us to classify cellular responses into distinct mechanistic categories. If DFT1 cells exhibit increased stiffness accompanied by a rise in tCho levels, it suggests that cytoskeletal repair mechanisms are activated as a resistance strategy. Alternatively, if there is a decrease in both stiffness and tCho levels, the cytoskeleton will have been disrupted with no compensation – indicative of successful treatment.

Table 1: Interpretation of possible findings generated from this study. The stiffness and tCho levels are in comparison to the cells' measurements prior to vincristine treatment. These findings are in reference to either the DFTD or neuroblastoma cells during treatment in order to compare these findings between susceptible and semi-resistant cell types.

Findings		**What it indicates**
Cell stiffness (AFM)	**tCho levels (MRS)**	
No change	No change	No effect from vincristine treatment. Cells are completely resistant to vincristine's mechanism of action.
No change	Increase	Metabolic adaptation to vincristine treatment – the cells could be reinforcing their cytoskeleton due to vincristine treatment.
No change	Decrease	Stable cytoskeleton, but early signs of stress seen in cell metabolism – likely inducing apoptosis.
Increase	No change	Resistance to vincristine has occurred, but not because of obvious cell reinforcement (because the metabolic profile is unchanged). Indicates that resistance lies in something other than cell

		metabolism defense mechanisms.
Increase	Increase	Resistance to vincristine shown, with compensation via cytoskeletal repair evident from the changed metabolic profile – this is an adaptive response to vincristine treatment that is a likely explanation of the cell's semi-resistance.
Increase	Decrease	Inconclusive – potentially the cell is running out of resources to repair and showing early signs of apoptosis, but resistance to vincristine has still been displayed through its stiffening.
Decrease	No change	Cytoskeleton is successfully destabilized, with no metabolic response. The cytoskeleton is weakened but there are no signs of apoptosis at this point.
Decrease	Increase	Cytoskeleton is successfully destabilized and there are compensatory measures taken – cell is attempting to regenerate/reinforce the cytoskeleton in light of destabilization. This repair mechanism may explain the partial resistance of cells.
Decrease	Decrease	Successful treatment – cytoskeleton has been destabilized and there is a metabolic decline suggesting apoptosis/stress-induced cell death.

By comparing the DFT1 and neuroblastoma cell responses, this study will highlight whether DFT1 cells' resistance to vincristine is driven by their cytoskeleton's ability to adapt. As well, the time marks that this study covers will identify periods of susceptibility in the DFT1 cells, opening possibilities to combination therapy. Identifying this could inform future treatment strategies and research pathways for DFTD, as well as chemotherapy-resistant cancers at large. By understanding the cytoskeleton's role in DFT1

treatment, we can gain a better understanding of how structural adaptations contribute to drug resistance, and where future opportunities lie in DFTD therapeutics.

Imaging and Spectroscopy

For our experimental study, we make use of magnetic resonance spectroscopy (MRS) for data collection. We will use ^{1}H-MRS to measure tCho concentrations and compare the results between our non-treated and treated human neuroblastoma and DFT1 cells. Its selection was based on a few particular advantages it has over nuclear magnetic resonance spectroscopy (NMR) and magnetic resonance imaging (MRI). NMR produces resonance spectroscopies of greater resolution which could cause resonance overlap when trying to analyze a chemically diverse sample such as a cell. MRI lacks the capability to identify specific metabolites and will instead show areas of high proton density within our samples.[55] Thus, the best choice for our cellular stiffness and metabolism study is MRS.

Nuclear species used for MRS, NMR, and MRI data collection must have an odd-numbered atomic mass as this gives them the property of angular momentum; also known as “spin”. This spin is quantized and described with the second quantum number I. Nuclei that exhibit spin also possess a magnetic dipole moment whose vector points parallel or antiparallel to the spin vector.[56] However, the direction and magnitude of the spin vector can be described with the quantum number M_I, with the maximum possible configurations given by 2I+1. Under the absence of a magnetic field, each M_I is the same energy level. This means that nuclear magnetic dipole vectors can exist in 2I+1 many orientations and freely switch between them. MRS takes advantage of these properties by establishing net polarization of the nuclear species that we are interested in through the influence of an external magnetic field.[57] This net

polarization induces Zeeman splitting which describes how different M_I values become separate in energy level.

The nuclei spin vectors move circularly and around the magnetic field vectors in a motion called precession.[56] This precession is caused by small torques applied to the nucleus that arise due to the interaction between the nuclear magnetic dipole and the magnetic field.[58] The rate of this precession is called the Larmor frequency and occurs at a constant angle when there are no energy transitions. The Larmor frequency of a nucleus depends on its own inherent properties as well as the strength of the external magnetic field as implied in Equation 8,

$$\omega = \gamma B_m \tag{8}$$

where ω is the Larmor Frequency, B_m is the strength of the external magnetic field, and γ is the gyromagnetic ratio. γ is derived from the ratio of the nuclear magnetic moment and total angular momentum.[59] As the net polarization is caused by the interaction between the nuclear magnetic moment and the external magnetic field, γ describes how "responsive" the nuclear magnetic moment is relative to its spin. This is because the small magnetic torques experienced by the nucleus will also change its spin. γ keeps the Larmor frequency calculations relative to the unique physical characteristic of different nuclei. The Larmor frequency also describes the frequency of electromagnetic disturbance required to induce M_I quantum state energy transitions, or nuclear resonance. These nuclei can undergo energy state transitions by their interaction with electromagnetic radio frequencies (RF).[59] The exact frequency of these photons must match the Larmor frequency of the nuclei being excited. This is a consequence of the Zeeman effect, thus the Larmor frequency corresponds to the discrete energy gap between M_I spin states.[60]

In practice, the sample is subjected to a series of RF pulses to induce this excitation. Once the RF pulses stop, the nuclei will precess towards their ground M_I state causing perturbations in the external magnetic field. Specialized sensors called Faraday induction sensors in MRS machines will detect these magnetic fluxes by exploiting Faraday's law of induction; converting the disturbances to electrical current.[59] The resultant current oscillates at the same frequency as the magnetic fluxes which are interpreted by a computer. These sinusoidal signals are called free induction decay signals (FID) because over time, the amplitudes will decrease at the Larmor frequency, reflecting the quantum behaviour of the nuclei as they transition towards ground state.[57] To convert this information into interpretable data, a Fourier transform is applied to break down the FID signal into individual composite signals. Naturally, the raw FID signal will also oscillate between negative and positive so a correction is applied by the computer to represent all negative phases as positive.

The resulting magnetic resonance spectrum displays data along an x axis that corresponds to parts-per-million shifts in frequency (ppm), which describes the differences in frequencies among spectral peaks. Varying frequencies arise by the chemical environment of the nucleus such as the presence of electrons. Electrons propagate their own magnetic field, which can cause variation in their corresponding nucleus's resonance. Each peak corresponds to a different chemical present in the sample and their concentrations can be measured by integrating the area under them.[61]

We will make use of ^{1}H MRS which involves resonating particularly hydrogen nuclei. We aim to resonate the hydrogen atoms in the trimethylammonium headgroups of major mobile choline-containing phospholipid metabolites.[53] The total choline (tCho) resonance peak appears at 3.2 ppm and serves as a biomarker for membrane metabolism as shown in Figure 6.

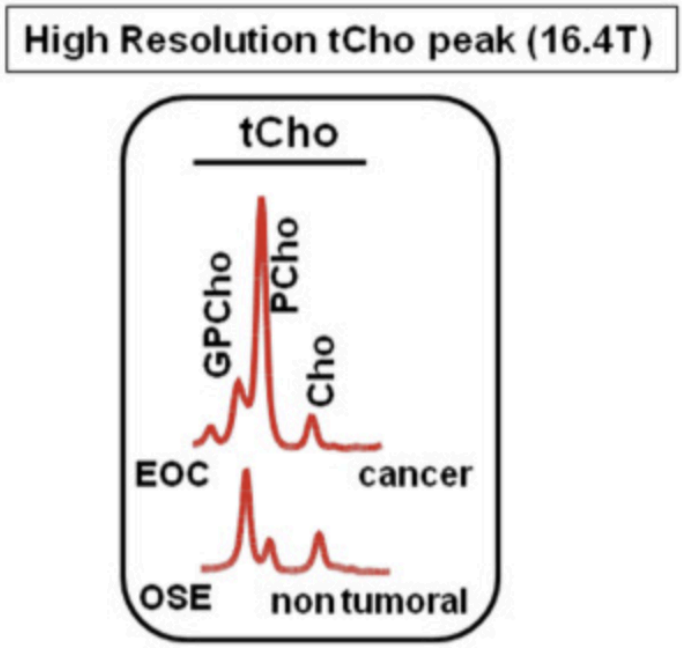

Figure 6: Comparing tCho peaks between cancerous epithelial ovarian cells and non-cancerous ovarian surface epithelial cells under a high resolution ^{1}H-MRS resonance spectrum. In the cancerous cells, the tCho peaks in the cancerous tissue are taller and wider relative to the non-cancerous cells.[53]

This application of ^{1}H MRS will allow us to gain insight on the structural effects of vincristine by analyzing the change in concentration of choline metabolites associated with structural stress adaptation. Choline kinase is an enzyme involved in catalyzing a reaction that yields phosphocholine (pCho); the precursor of the most abundant phospholipid in mammalian cell membranes, phosphatidylcholine.[62] If our magnetic resonance spectra show broadened or increased tCho peak heights following administration, then we can interpret this as choline kinase being upregulated. This signifies that the structural effect that vincristine has on the cytoskeleton is not sufficient in stimulating apoptosis. However, if the total area under tCho peaks is reduced, then we can assume that choline kinase has been downregulated which signifies that the cell is preparing to undergo apoptosis.[63] As our study will monitor these cells over the

course of 48 hours, ^{1}H MRS scans will occur every 6 hours until 24 hours, to which our next check up will occur at 48 hours. This ensures that any second waves of apoptosis are detected, especially following initial tCho spikes.

Conclusions and Perspectives

DFTD threatens to eradicate the entirety of the Tasmanian devil population through its rapid transmission and its high mortality, making it fatal to every devil it infects. Chemotherapeutic drugs, particularly vincristine, are often employed as the first method of treatment applied. Both the computational analysis and proposed study look to investigate the effectiveness of vincristine, its mechanism of action, and any deficiencies in its use as a treatment of DFTD. The computational study demonstrates the influence of chemotherapeutics upon tumour cell division using linear regression models, depicting the outcomes of tumour cell division with and without the presence of vincristine. From this analysis, we observe that vincristine has stopped DFTD cells from proliferating in an unpredictable manner. The effects of vincristine on final cell count is strong, with an R^2 value of 0.980. In contrast, DFTD cell proliferation without treatment was unpredictable and aggressive, with an R^2 value of 0.006, indicating very little to no correlation. Although vincristine administration was not suggestive of absolute tumour elimination, it is key in preventing excessive growth, indicating semi-resistance.

The proposed study explores this semi-resistance through vincristine's effects on DFT1 cell stiffness and potential alterations of choline metabolism in DFT1 during vincristine administration. These findings will contribute to our understanding of the cellular evasion of apoptosis and help us understand the biomechanical responses of DFT1 under chemotherapeutic stress. These findings will inform the ongoing attempts to treat DFTD with chemotherapeutics, indicating the possibility of combination therapies with

vincristine, the viability of chemotherapeutics in general, and the potential need for pivoting away from chemotherapy in DFTD treatment. This study integrates cell mechanics and biochemical processes through a multidisciplinary approach to investigate DFT1's evasion of apoptosis, bringing an important perspective to DFTD treatment progression and broader chemotherapeutic strategies.

While this study provides important insights into the biophysical mechanisms of DFTD, certain limitations must be acknowledged, along with opportunities for future research to expand on these findings. Considering this trial will be performed on cell lines, it may fall short in replicating active biological conditions and fail in addressing crucial external factors such as the environment. As well, this study will focus on DFT1 cells, and so future questions in DFT2 cellular response to vincristine will remain. A final limitation of the proposed study is the lack of focus on healthy Tasmanian devil cells undergoing vincristine treatment. If this study finds vincristine treatment – alone or in combination with other therapies – to be viable, future research must focus on the effects of vincristine on cytoskeletal integrity and choline metabolism in healthy Tasmanian devil cells. Additional research avenues stemming from this study include examining the interactions between elements of the cytoskeleton during and after potential repair, further refining our understanding of specific repair mechanisms. As well, using the cellular stiffness and tCho levels at each time mark may reveal lags in repair mechanisms, opening the door to combination therapies. This will be an important route to explore upon completion of this study.

In cancers without clear and successful treatment options such as DFTD, we must investigate all angles. By providing a biophysical perspective on DFTD's cellular defense mechanisms, this study will contribute to the broader understanding of cancer cell mechanics, offering insights that could inform future treatment strategies and advance cancer research.

References

1. McCallum H, Tompkins DM, Jones M, et al. Distribution and Impacts of Tasmanian Devil Facial Tumor Disease. *EcoHealth*. 2007;4(3):318-325. doi:10.1007/s10393-007-0118-0

2. Oliveira JT, Yanick C, Wein N, Gomez Limia CE. Neuron-Schwann cell interactions in peripheral nervous system homeostasis, disease, and preclinical treatment. *Front Cell Neurosci*. 2023;17. doi:10.3389/fncel.2023.1248922

3. Tovar C, Pye RJ, Kreiss A, et al. Regression of devil facial tumour disease following immunotherapy in immunised Tasmanian devils. *Sci Rep*. 2017;7(1):43827. doi:10.1038/srep43827

4. Loh R, Bergfeld J, Hayes D, et al. The Pathology of Devil Facial Tumor Disease (DFTD) in Tasmanian Devils (Sarcophilus harrisii). *Vet Pathol*. 2006;43(6):890-895. doi:10.1354/vp.43-6-890

5. McCallum H, Jones M, Hawkins C, et al. Transmission dynamics of Tasmanian devil facial tumor disease may lead to disease-induced extinction. *Ecology*. 2009;90(12):3379-3392. doi:10.1890/08-1763.1

6. Phalen DN, Frimberger AE, Peck S, et al. Doxorubicin and carboplatin trials in Tasmanian devils (*Sarcophilus harrisii*) with Tasmanian devil facial tumor disease. *Vet J*. 2015;206(3):312-316. doi:10.1016/j.tvjl.2015.10.013

7. Pye R, Patchett A, McLennan E, et al. Immunization Strategies Producing a Humoral IgG Immune Response against Devil Facial Tumor Disease in the Majority of Tasmanian Devils Destined for Wild Release. *Front Immunol*. 2018;9:259. doi:10.3389/fimmu.2018.00259

8. Li X, Wang J. Mechanical tumor microenvironment and transduction: cytoskeleton mediates cancer cell invasion and metastasis. *Int J Biol Sci*. 2020;16(12):2014-2028. doi:10.7150/ijbs.44943

9. Stylianou A, Mpekris F, Voutouri C, et al. Nanomechanical properties of solid tumors as treatment monitoring biomarkers. *Acta Biomater*. 2022;154:324-334. doi:10.1016/j.actbio.2022.10.021

10. Škubník J, Pavlíčková VS, Ruml T, Rimpelová S. Vincristine in Combination Therapy of Cancer: Emerging Trends in Clinics. *Biology*. 2021;10(9):849. doi:10.3390/biology10090849

11. Alhalhooly L, Mamnoon B, Kim J, Mallik S, Choi Y. Dynamic cellular biomechanics in responses to chemotherapeutic drug in hypoxia probed by atomic force spectroscopy. *Oncotarget*. 2021;12(12):1165-1177. doi:10.18632/oncotarget.27974

12. Aubrey BJ, Kelly GL, Janic A, Herold MJ, Strasser A. How does p53 induce apoptosis and how does this relate to p53-mediated tumour suppression? *Cell Death Differ*. 2018;25(1):104-113. doi:10.1038/cdd.2017.169

13. Tu Y, Cheng S, Zhang S, Sun H, Xu Z. Vincristine induces cell cycle arrest and apoptosis in SH-SY5Y human neuroblastoma cells. *Int J Mol Med*. 2013;31(1):113-119. doi:10.3892/ijmm.2012.1167

14. Dhyani P, Quispe C, Sharma E, et al. Anticancer potential of alkaloids: a key emphasis to colchicine, vinblastine, vincristine, vindesine, vinorelbine and vincamine. *Cancer Cell Int*. 2022;22(1):206. doi:10.1186/s12935-022-02624-9

15. Ma S, Li M, Liu N, et al. Vincristine liposomes with smaller particle size have stronger diffusion ability in tumor and improve tumor accumulation of vincristine significantly. *Oncotarget*. 2017;8(50):87276-87291. doi:10.18632/oncotarget.20162

16. Mo X, Rao DP, Kaur K, et al. Indole Derivatives: A Versatile Scaffold in Modern Drug Discovery—An Updated Review on Their Multifaceted Therapeutic Applications (2020–2024). *Molecules*. 2024;29(19):4770. doi:10.3390/molecules29194770

17. Lobert S, Vulevic B, Correia JJ. Interaction of Vinca Alkaloids with Tubulin: A Comparison of Vinblastine, Vincristine, and Vinorelbine. *Biochemistry*. 1996;35(21):6806-6814. doi:10.1021/bi953037i

18. Zhang T, Zheng Y, Peng Q, Cao X, Gong T, Zhang Z. A novel submicron emulsion system loaded with vincristine–oleic acid ion-pair complex with improved anticancer effect: in vitro and in vivo studies. *Int J Nanomedicine*. 2013;8:1185-1196. doi:10.2147/IJN.S41775

19. Phalen DN, Frimberger A, Pyecroft S, et al. Vincristine Chemotherapy Trials and Pharmacokinetics in Tasmanian Devils with Tasmanian Devil Facial Tumor Disease. *PLOS ONE*. 2013;8(6):e65133. doi:10.1371/journal.pone.0065133

20. Medina-Vogel G. Emerging Infectious Diseases of Wildlife and Species Conservation. *Microbiol Spectr*. 2013;1(2):10.1128/microbiolspec.oh-0004-2012. doi:10.1128/microbiolspec.oh-0004-2012

21. Jones ME, Hamede R, Storfer A, Hohenlohe P, Murchison EP, McCallum H. Emergence, transmission and evolution of an uncommon enemy: Tasmanian devil facial tumour disease. In: Fenton A, Tompkins D, Wilson K, eds. *Wildlife Disease Ecology: Linking Theory to Data and Application*. Ecological Reviews. Cambridge University Press; 2019:321-341. doi:10.1017/9781316479964.011

22. Stammnitz MR, Gori K, Kwon YM, et al. The evolution of two transmissible cancers in Tasmanian devils. *Science*. 2023;380(6642):283-293. doi:10.1126/science.abq6453

23. Patchett AL, Flies AS, Lyons AB, Woods GM. Curse of the devil: molecular insights into the emergence of transmissible cancers in the Tasmanian devil (Sarcophilus harrisii). *Cell Mol Life Sci CMLS*. 2020;77(13):2507-2525. doi:10.1007/s00018-019-03435-4

24. Hollings T, Jones M, Mooney N, Mccallum H. Trophic Cascades Following the Disease-Induced Decline of an Apex Predator, the Tasmanian Devil. *Conserv Biol*. 2014;28(1):63-75. doi:10.1111/cobi.12152

25. van Vuuren RJ, Visagie MH, Theron AE, Joubert AM. Antimitotic drugs in the treatment of cancer. *Cancer Chemother Pharmacol*. 2015;76(6):1101-1112. doi:10.1007/s00280-015-2903-8

26. Storfer A, Hohenlohe PA, Margres MJ, et al. The devil is in the details: Genomics of transmissible cancers in Tasmanian devils. *PLoS Pathog*. 2018;14(8):e1007098. doi:10.1371/journal.ppat.1007098

27. Orth JD, Loewer A, Lahav G, Mitchison TJ. Prolonged mitotic arrest triggers partial activation of apoptosis, resulting in DNA damage and p53 induction. *Mol Biol Cell*. 2012;23(4):567-576. doi:10.1091/mbc.e11-09-0781

28. Torrino S, Grasset EM, Audebert S, et al. Mechano-induced cell metabolism promotes microtubule glutamylation to force metastasis. *Cell Metab*. 2021;33(7):1342-1357.e10. doi:10.1016/j.cmet.2021.05.009

29. Podo F, Paris L, Cecchetti S, et al. Activation of Phosphatidylcholine-Specific Phospholipase C in Breast and Ovarian Cancer: Impact on MRS-Detected Choline Metabolic Profile and Perspectives for Targeted Therapy. *Front Oncol*. 2016;6. doi:10.3389/fonc.2016.00171

30. Foster DA, Xu L. Phospholipase D in Cell Proliferation and Cancer1. *Mol Cancer Res*. 2003;1(11):789-800.

31. Najera J, Rosenberger MR, Datta M. Atomic Force Microscopy Methods to Measure Tumor Mechanical Properties. *Cancers*. 2023;15(13):3285. doi:10.3390/cancers15133285

32. Li QS, Lee GYH, Ong CN, Lim CT. AFM indentation study of breast cancer cells. *Biochem Biophys Res Commun*. 2008;374(4):609-613. doi:10.1016/j.bbrc.2008.07.078

33. Li M, Xiao X, Liu L, Xi N, Wang Y. Nanoscale Quantifying the Effects of Targeted Drug on Chemotherapy in Lymphoma Treatment Using Atomic Force Microscopy. *IEEE Trans Biomed Eng*. 2016;63(10):2187-2199. doi:10.1109/TBME.2015.2512924

34. Burr ML, Sparbier CE, Chan KL, et al. An Evolutionarily Conserved Function of Polycomb Silences the MHC Class I Antigen Presentation Pathway and Enables Immune Evasion in Cancer. *Cancer Cell*. 2019;36(4):385-401.e8. doi:10.1016/j.ccell.2019.08.008

35. Penet MF, Sharma RK, Bharti S, Mori N, Artemov D, Bhujwalla ZM. Cancer insights from magnetic resonance spectroscopy of cells and excised tumors. *NMR Biomed*. 2023;36(4):e4724. doi:10.1002/nbm.4724

36. Schneider F, Colin-York H, Fritzsche M. Quantitative Bio-Imaging Tools to Dissect the Interplay of

Membrane and Cytoskeletal Actin Dynamics in Immune Cells. *Front Immunol*. 2021;11:612542. doi:10.3389/fimmu.2020.612542

37. Sharma U, Jagannathan NR. In vivo MR spectroscopy for breast cancer diagnosis. *BJR|Open*. 2019;1(1):20180040. doi:10.1259/bjro.20180040

38. Radermacher KA, Magat J, Bouzin C, et al. Multimodal assessment of early tumor response to chemotherapy: comparison between diffusion-weighted MRI, 1H-MR spectroscopy of choline and USPIO particles targeted at cell death. *NMR Biomed*. 2012;25(4):514-522. doi:10.1002/nbm.1765

39. Cheng M, Bhujwalla ZM, Glunde K. Targeting Phospholipid Metabolism in Cancer. *Front Oncol*. 2016;6. doi:10.3389/fonc.2016.00266

40. Kothari A, Hittelman WN, Chambers TC. Cell Cycle–Dependent Mechanisms Underlie Vincristine-Induced Death of Primary Acute Lymphoblastic Leukemia Cells. *Cancer Res*. 2016;76(12):3553-3561. doi:10.1158/0008-5472.CAN-15-2104

41. Pinfold TL, Brown GK, Bettiol SS, Woods GM. Mouse Model of Devil Facial Tumour Disease Establishes That an Effective Immune Response Can be Generated Against the Cancer Cells. *Front Immunol*. 2014;5:251. doi:10.3389/fimmu.2014.00251

42. Kaya ZB, Santiago-Padilla V, Lim M, Boschen SL, Atilla P, McLean PJ. Optimizing SH-SY5Y cell culture: exploring the beneficial effects of an alternative media supplement on cell proliferation and viability. *Sci Rep*. 2024;14(1):4775. doi:10.1038/s41598-024-55516-5

43. Peet AC, McConville C, Wilson M, et al. 1H MRS identifies specific metabolite profiles associated with MYCN-amplified and non-amplified tumour subtypes of neuroblastoma cell lines. *NMR Biomed*. 2007;20(7):692-700. doi:10.1002/nbm.1181

44. Divakarraju PV, Pandurangan V, Nithyadharan M. Atomic force microscopy-based nanoindentation technique for characterizing the transverse and shear moduli of flax fibers. *Compos Sci Technol*. 2024;258:110890. doi:10.1016/j.compscitech.2024.110890

45. Chung YL. Magnetic Resonance Spectroscopy (MRS)-Based Methods for Examining Cancer Metabolism in Response to Oncogenic Kinase Drug Treatment. In: Tan AC, Huang PH, eds. *Kinase Signaling Networks*. Springer; 2017:393-404. doi:10.1007/978-1-4939-7154-1_25

46. Le Gall G. Sample Collection and Preparation of Biofluids and Extracts for NMR Spectroscopy. In: Bjerrum JT, ed. *Metabonomics: Methods and Protocols*. Springer; 2015:15-28. doi:10.1007/978-1-4939-2377-9_2

47. Aranibar N, Reily MD. NMR Methods for Metabolomics of Mammalian Cell Culture Bioreactors. In: Pörtner R, ed. *Animal Cell Biotechnology: Methods and Protocols*. Humana Press; 2014:223-236. doi:10.1007/978-1-62703-733-4_15

48. Sapcariu SC, Kanashova T, Weindl D, Ghelfi J, Dittmar G, Hiller K. Simultaneous extraction of proteins and metabolites from cells in culture. *MethodsX*. 2014;1:74-80. doi:10.1016/j.mex.2014.07.002

49. Thomas G, Burnham NA, Camesano TA, Wen Q. Measuring the Mechanical Properties of Living Cells Using Atomic Force Microscopy. *J Vis Exp JoVE*. 2013;(76):e50497. doi:10.3791/50497

50. Li QS, Lee GYH, Ong CN, Lim CT. AFM indentation study of breast cancer cells. *Biochem Biophys Res Commun*. 2008;374(4):609-613. doi:10.1016/j.bbrc.2008.07.078

51. Tilleman TR, Tilleman MM, Neumann MHA. The elastic properties of cancerous skin: Poisson's ratio and Young's modulus. *Isr Med Assoc J IMAJ*. 2004;6(12):753-755.

52. Shao W, Gu J, Huang C, et al. Malignancy-associated metabolic profiling of human glioma cell lines using 1H NMR spectroscopy. *Mol Cancer*. 2014;13(1):197. doi:10.1186/1476-4598-13-197

53. Iorio E, Podo F, Leach MO, Koutcher J, Blankenberg FG, Norfray JF. A novel roadmap connecting the 1H-MRS total choline resonance to all hallmarks of cancer following targeted therapy. *Eur Radiol Exp*. 2021;5:5. doi:10.1186/s41747-020-00192-z

54. Hanspach J, Nagel AM, Hensel B, Uder M, Koros L, Laun FB. Sample size estimation: Current practice and considerations for original investigations in MRI technical development studies. *Magn Reson Med*. 2021;85(4):2109-2116. doi:10.1002/mrm.28550

55. Wilson M, Andronesi O, Barker PB, et al. A Methodological Consensus on Clinical Proton MR Spectroscopy of the Brain: Review and Recommendations. *Magn Reson Med*. 2019;82(2):527-550. doi:10.1002/mrm.27742

56. Levitt M. *Spin Dynamics: Basics of Nuclear Magnetic Resonance*. Vol 40. John Wiley & Sons; 2002. Accessed April 3, 2025. https://onlinelibrary.wiley.com/doi/abs/10.1002/mrc.1092

57. Tognarelli JM, Dawood M, Shariff MIF, et al. Magnetic Resonance Spectroscopy: Principles and Techniques: Lessons for Clinicians. *J Clin Exp Hepatol*. 2015;5(4):320-328. doi:10.1016/j.jceh.2015.10.006

58. Conradi MS. Understanding magnetic fields, for NMR/MRI. *J Magn Reson Open*. 2024;20:100158. doi:10.1016/j.jmro.2024.100158

59. Kraus R, Espy M, Magnelind P, Volegov P. *Ultra-Low Field Nuclear Magnetic Resonance: A New MRI Regime*. Oxford University Press; 2014.

60. Wexler AD, Woisetschläger J, Reiter U, et al. Nuclear Magnetic Relaxation Mapping of Spin Relaxation in Electrically Stressed Glycerol. *ACS Omega*. 2020;5(35):22057-22070. doi:10.1021/acsomega.0c02059

61. Schoenberger T, Menges S, Bernstein MA, et al. Improving the Performance of High-Precision qNMR Measurements by a Double Integration Procedure in Practical Cases. *Anal Chem*. 2016;88(7):3836-3843. doi:10.1021/acs.analchem.5b04911

62. Ridgway ND. Chapter 7 - Phospholipid Synthesis in Mammalian Cells. In: Ridgway ND, McLeod RS, eds. *Biochemistry of Lipids, Lipoproteins and Membranes (Sixth Edition)*. Elsevier; 2016:209-236. doi:10.1016/B978-0-444-63438-2.00007-9

63. Arlauckas SP, Popov AV, Delikatny EJ. Choline kinase alpha—Putting the ChoK-hold on tumor metabolism. *Prog Lipid Res*. 2016;63:28-40. doi:10.1016/j.plipres.2016.03.005